

Treatment of purified terephthalic acid wastewater using a bio-waste-adsorbent bagasse fly ash (BFA)

Shilpi Verma^{1,2} · Basheshwar Prasad¹ · Indra Mani Mishra¹

Received: 18 July 2016 / Accepted: 24 October 2016 / Published online: 31 October 2016
© Springer-Verlag Berlin Heidelberg 2016

Abstract Purified terephthalic acid (PTA) plant of a petrochemical unit generates wastewater having high pollution load. Acid treatment of this wastewater reduces the chemical oxygen demand (COD) load by more than 50%, still leaving substantial COD load (>1500 mg/L) which should be removed. The present study reports on the use of a bio-waste-adsorbent bagasse fly ash (BFA) for the reduction of COD and other recalcitrant acids from this wastewater. The BFA showed basic character and was mesoporous with a BET specific surface area of 82.4 m²/g. Optimum conditions for the adsorptive treatment of acid-pretreated PTA wastewater were found to be as follows: initial pH (pH_i) = 4, BFA dosage = 15 g/L, and contact time = 3 h. Adsorption treatment resulted in 58.2% removal of COD, 96.3% removal of terephthalic acid (TA), and 99.9% removal of benzoic acid (BA). TA and BA were removed from the pretreated PTA wastewater through precipitation and sedimentation of undissociated acid molecules inside the mesopores of the BFA. The results showed that the COD removed by the BFA followed pseudo-second-order kinetics. Equilibrium sorption data were best correlated by the Freundlich isotherm. The process of adsorptive removal of COD was found to be exothermic. The change in the Gibbs free energy was found to be negative,

suggesting that the adsorption process is spontaneous and feasible for the treatment of PTA wastewater.

Keywords Adsorption thermodynamics · BFA · Isotherms · Kinetics · Petrochemical wastewater

Introduction

During petroleum and natural gas processing, a number of aromatics are formed. One such aromatic compound, para (*p*-) xylene is used as a feedstock for the manufacture of the purified terephthalic acid (PTA). The PTA manufacturing consists of two separate processes, the catalytic air oxidation of *p*-xylene with bromine as a co-promoter to produce crude terephthalic acid (TA) and the catalytic hydrogenation of the TA and subsequent crystallization. PTA is the basic raw material for the manufacture of polyester including polyethylene terephthalate (PET) bottle resin, fiber, and polyester film. The rest of the PTA is used in making terephthaloyl chloride, elastomers, plasticisers, and liquid crystal polymers (Wittcoff et al. 2004; Pophali et al. 2007; Verma et al. 2014a; Joung et al. 2009).

The PTA manufacturing process produces 3 to 10 m³ of wastewater per ton of PTA produced with a COD load of 5–20 kg COD/m³ of wastewater. This wastewater contains a number of chemicals and aromatics. While benzoic acid (BA), *p*-toluic acid, 4-carboxybenzaldehyde (4-CBA), phthalic acid (PA), and terephthalic acid (TA) are the major components, methyl acetate, 4-formylbenzoic acid, and *p*-xylene are the minor components. About 70–80% of COD is contributed by major components (Kleerebezem et al. 1999a, 1999b; Pophali et al. 2007; Zhang et al. 2010).

The PTA and its products affect adversely the human reproductive and developmental systems. Some of the products

Responsible editor: Angeles Blanco

✉ Shilpi Verma
shilpi.env@gmail.com

¹ Department of Chemical Engineering, Indian Institute of Technology Roorkee, Roorkee 247667, India

² Present address: Department of Chemical Engineering, Indian Institute of Technology Guwahati, Guwahati, Assam 781039, India

such as phthalates, esters of PTA, and their intermediate degradation products have teratogenic, carcinogenic, and endocrine-disrupting properties (Hauser and Calafat 2005; Heudorf et al. 2007; Swan 2008; Lyche et al. 2009; Meeker et al. 2009). Due to the inherent toxicity of phthalates, it is essential to treat the PTA wastewater so as to reduce its pollution load within the prescribed limit. The Ministry of Environment and Forest (MoEF), Government of India, has prescribed the effluent discharge limits from a petrochemical plant into sewer system in terms of COD and biological oxygen demand (BOD): COD \leq 125 mg/L and BOD \leq 50 mg/L.

The wastewaters containing hazardous substances have been traditionally treated using various physico-chemical treatment methods. The physico-chemical treatment processes include adsorption (Tsang et al. 2008; Dulazi and Liu 2011), coagulation and flocculation (Wen et al. 2006; Karthik et al. 2008; Verma et al. 2010), acid precipitation (Garg et al. 2010; Verma et al. 2014a), and advanced oxidation processes (Park et al. 2003; Thiruvengkatachari et al. 2007; Pillai et al. 2009; Shafaei et al. 2010). The adsorption process is an efficient treatment technique for the removal of many bio-recalcitrant chemical substances. The adsorption process does not produce any by-products during treatment, although the spent adsorbents need to be either regenerated for cyclic treatment or disposed off and managed in an eco-friendly manner.

Various adsorbents which have been used in the treatment of phthalates and their esters include modified activated carbon (Adhoum and Monser 2004), activated carbon cloth (Ayranci and Duman 2006), chitosan and α -cyclodextrin-linked chitosan beads (Chen and Chung 2006, Chen et al. 2007), granular activated carbons (GAC) (Tsang et al. 2008), carbon having micropores (Long et al. 2009), different polymeric resins (Xu et al. 2011), and chitosan beads containing immobilized lipase (Dulazi and Liu 2011). However, to the best of the authors' knowledge, only few studies have been reported on the removal of TA from aqueous solution. Anbia and Salehi (2012) synthesized polyelectrolyte-modified ordered mesoporous carbon (CMK1/PDDA) for the adsorptive removal of 4-carboxybenzaldehyde, *p*-toluic acid, BA, PA, and TA from PTA wastewater. TiO₂ nanoparticles were used to remove TA by Caliskan et al. (2013).

A cost-effective adsorbent with high adsorption capacity, fast kinetics with a simple regeneration and/or disposal method, can make the adsorptive treatment of PTA wastewater an attractive proposition. Bio-waste materials like bagasse fly ash (BFA) have proved to be very efficient adsorbents for the removal of a number of hazardous components like phenol and its derivatives (Srivastava et al. 2006a), pyridine and picoline, and metal ions (Lataye et al. 2006, 2008).

This paper examines the effectiveness of BFA for the adsorptive removal of pollutants (COD is taken as the gross measure of pollution load in the present study) from PTA wastewater. The PTA wastewater used in the adsorption

studies was pretreated with sulfuric acid. The acidification of several industrial effluents led to the precipitation of many organic/inorganic components present in them with a COD removal efficiency of >50% (Gilarranz et al. 1998; Rivas et al. 2004; Garg et al. 2010; Verma et al. 2014a). The present study concentrated on those variables which affect the COD removal by the adsorptive treatment of PTA. The equilibrium adsorption characteristics and kinetics have also been studied. Freundlich, Langmuir, and Temkin equations have been used to test their validity for the experimental equilibrium sorption data. To understand the effect of COD concentration on the isosteric heat of adsorption, thermodynamic studies were also conducted. A comparative assessment of adsorptive performance of BFA and GAC for the treatment of PTA wastewater is also presented.

Materials and methods

PTA wastewater

The PTA wastewater treatment plant was used as the source of PTA wastewater, collected from the flow equalization tank unit. The PTA wastewater treatment plant was located in Northern India. It was stored at 4 °C in the laboratory cold storage and used as obtained.

Adsorbent

The BFA was collected from a nearby sugar mill (Northern India), a steam-generating unit, and screened. This bio-waste was cleaned of dirt by hot water washing and then sun-dried and sieved through standard screens on a sieve shaker. The fraction with an average particle size of 0.45 mm was used in the experiments. Standard methods were used for the physico-chemical characterization of BFA.

IS: 1350–1984, part I (standard procedure) was used to carry out the proximate analysis of BFA. Solid addition method was used to determine the zero surface charge characteristics of the BFA (Srivastava et al. 2006b). The surface functional groups on the virgin BFA were studied by using Fourier transform infrared spectroscopy (FTIR, Nicolet Avatar 370, USA). The Boehm titration method was employed for the quantification of the functional groups present on the virgin BFA surface (Nevskaia et al. 2004).

The specific surface area of the BFA was found out by nitrogen adsorption at 77 K using ASAP 2020 Physisorption Analyzer (Micromeritics, USA). The pore size distribution curve for BFA was determined using the BJH model (Barrett et al. 1951).

Scanning electron microscopy (SEM) of the BFA was carried out with a scanning electron microscope (LEO 435VP, England) operating with an SE1 detector. Energy-dispersive

X-ray (EDX) spectroscopy (FE-SEM QUANTA 200 FEG) was carried out to determine the elemental composition of the BFA.

Experimentation

The pH of the wastewater was reduced to 4, 3, and 2 after treating with 1 M H₂SO₄ for 20 min with a constant stirring at 200 revolutions per minute over the temperature range of 288–323 K. This results in the precipitation of organics/inorganics from the wastewater. Due to acid precipitation, the concentration of TA, BA, and COD reduced from 299, 275, and 3530 mg/L to 27.3, 109.3, and 1650 mg/L, respectively. The resultant mixture was filtered using a Whatman filter paper, with a pore size of 11 μm (Sigma Aldrich Z274852), and the filtrate was subsequently subjected to the adsorption experiments. The details of acid precipitation are reported elsewhere (Verma et al. 2014a).

At the optimum pH_i and temperature 298 K, the BFA dosage was varied in the range of 5–40 g/L. The effect of pH_i was studied in the range of 2–10. The pH_i of the adsorbate solution was adjusted using either 1 M H₂SO₄ or 1 M NaOH. Standard methods were used for the analysis of various physico-chemical parameters of the wastewater (APHA 2003). The concentration of TA and BA was analyzed through HPLC (Park et al. 2003). The pollution load of the wastewater and the treated water was measured in terms of chemical oxygen demand (COD) using a COD analyzer (Aqualytic, Germany). The experiments were run in duplicate under the same experimental conditions, and the average of the two experimental runs is reported.

The absorptive COD removal was expressed in terms of percentage COD removal using the following relationship:

$$\%COD \text{ removal} = \frac{C_0 - C_e}{C_0} \times 100 \tag{1}$$

where C₀ represents the initial COD value (mg/L) and C_e, the equilibrium COD value (mg/L).

Kinetic parameters were determined at an optimum dosage of BFA and at optimum pH_i. The amount of adsorbate adsorbed, q_t (mg/g), at any time *t* was calculated as:

$$q_t = \frac{C_0 - C_t}{w} \times V \tag{2}$$

where COD value (mg/L) at time *t* (min) is represented by C_t, volume of the solution (L) is represented by V, and mass of the BFA (g) is represented by w.

To understand the effect of temperature on adsorption, isothermal adsorption experiments were performed at 298, 308, and 318 K with C₀ values ranging between 1650 and 165 mg/L at optimum pH_i and dosage of BFA for 3 h. The COD value of supernatant at equilibrium (C_e) was analyzed after the BFA was separated from the wastewater. The q_e (mg/g) was

calculated by using the following relationship:

$$q_e = \frac{C_0 - C_e}{w} \times V \tag{3}$$

where q_e (mg/g) is the equilibrium adsorption uptake.

Adsorption kinetic model

The prediction of kinetics is important for the prediction of adsorption rates and for the designing and modeling of the adsorbers. The pseudo-first-order model, pseudo-second-order model, and the intraparticle diffusion model were used to determine the mechanism of adsorption and potential rate controlling steps (Srivastava et al. 2006a; Srivastava et al. 2006b). Since the experiments were performed at 200 rpm, the external mass transfer effects were assumed to be absent.

Adsorption kinetic data could be treated by models given by Boyd et al. 1947, which is valid under the experimental conditions used. For adsorption particles of spherical shape, the solution of the simultaneous differential and algebraic equations leads to

$$F(t) = 1 - \frac{6}{\pi^2} \sum_{z=1}^{\infty} \frac{1}{z^2} \exp\left[\frac{-z^2 \pi^2 t D_e}{R_a^2}\right] \tag{4}$$

where F(t) = q_t/q_e, R is the radius of the BFA (m), D_e is the effective diffusion coefficient of COD in the BFA (m²/s), and z is an integer.

For the whole range of the F(t) from 0 to 1, Vermeulen (1953) gave an approximate equation as:

$$F(t) = \left[1 - \exp\left(\frac{-\pi^2 t D_e}{R_a^2}\right)\right]^{1/2} \tag{5}$$

This equation could further be simplified as:

$$\ln\left[\frac{1}{1 - (t)F^2}\right] = \frac{\pi^2 t D_e}{R_a^2} \tag{6}$$

where D_e can be determined from the slope of plot between ln[1/(1-F²(t))] and *t*.

Adsorption isotherm equations

The equilibrium adsorption data were plotted so as to determine the adsorption capacity of the BFA. The Langmuir, Freundlich, and Temkin isotherm equations were used to check their validity. These model equations, their parametric values and the deviations in terms of correlation coefficient, r², and the error function, residual sum of squares (RSS) are given in Table 4. The isotherm details and the significance of parameters are discussed elsewhere (Srivastava et al. 2006a; Verma et al. 2014a).

Adsorption thermodynamics

Using the change in the adsorption equilibrium constant (K_D) with T and the thermodynamic relations, one can calculate Gibbs free energy change (ΔG^0), entropy change (ΔS^0), and enthalpy change (ΔH^0), as given below:

$$\ln K_D = \frac{-\Delta G^0}{RT} = \frac{\Delta S^0}{R} - \frac{\Delta H^0}{RT} \quad (7)$$

where T is the absolute temperature (K), R the universal gas constant (8.314×10^{-3} kJ/mol K), ΔG^0 the Gibbs free energy change (kJ/mol), ΔH^0 the change in enthalpy (kJ/mol), ΔS^0 the entropy change (kJ/mol K), and $K_D (=q_e/C_e)$ the single point or linear sorption distribution coefficient. The changes in the enthalpy (ΔH^0) and entropy (ΔS^0) were obtained from the plot between $\ln K_D$ and $1/T$ (Srivastava et al. 2006a).

Isosteric enthalpy of adsorption

The Clausius-Clapeyron equation was used to determine the apparent isosteric heat of adsorption ($\Delta H_{st,a}$) at constant surface coverage (q_e)

$$\frac{d \ln C_e}{dT} = \frac{-\Delta H_{st,a}}{RT^2} \quad (8)$$

$$\Delta H_{st,a} = R \frac{d \ln C_e}{d \left(\frac{1}{T} \right)} |_{q_e} \quad (9)$$

The adsorption isotherm data at various temperatures can be used to determine the equilibrium concentration (C_e) for a specified value of adsorbed COD (Srivastava et al. 2007).

Result and discussion

A detailed discussion about COD, TA, and BA removal from PTA wastewater through acid precipitation is given elsewhere (Verma et al. 2014a). The concentration of the major components, TA and BA, in the acid-pretreated wastewater was found as TA = 27.3 mg/L, BA = 109.3 mg/L, and the COD = 1650 mg/L.

Characteristics of BFA: surface functional groups, structural morphology, texture, and porosity

The capacity of an adsorbent is strongly affected by the chemical structure of the surface of the adsorbents. Boehm titration was used to acquire the amount of numerous functional groups present on the surface of BFA (Boehm 1966), and the results are provided in Table 1. The method proposed by Zhuravlev (Zhuravlev 1987) to determine the density of

Table 1 Functional groups on the surface of the adsorbents quantified by Boehm's titration

Concentration of functional groups on surface (mmol/g)	BFA
Basic groups	1.18
Carboxylic group	0.03
Lactonic group	0.08
Phenolic group	0.02
Surface area concentration of functional groups (no. of molecules/m ²)	
Basic groups	8.4×10^{-3}
Carboxylic group	2.15×10^{-3}
Lactonic group	5.75×10^{-3}
Phenolic group	1.44×10^{-3}

various functional groups present on the surface of BFA was used in the present study. It was observed that both the basic and acidic functional groups were present on the BFA. The adsorption properties depend on the relative concentrations and properties of these functional groups. The results of Boehm titration show that the BFA is highly basic in nature (Table 1).

The presence of various functional groups on the surface of BFA is shown in FTIR spectra shown in Fig. 1. A broad band between 3200 and 3600 cm^{-1} indicates the presence of OH groups, both free and hydrogen bonded. This broad band indicates that the BFA surface has both the water and SiOH (silanol groups) (Abou-Mesalam 2000). Weak bands at 2920 and 2831 cm^{-1} indicate the asymmetric and symmetric C-H stretching of methylene groups, respectively. The presence of carbonate is indicated by the location of band at 1872 cm^{-1} . N-H in-plane bending of amide II functional group is represented at wavenumber 1580 cm^{-1} . The presence of the band at 1380 cm^{-1} shows the existence of carboxyl-carbonate structures. A strong band concentrated around 1093 cm^{-1} indicates

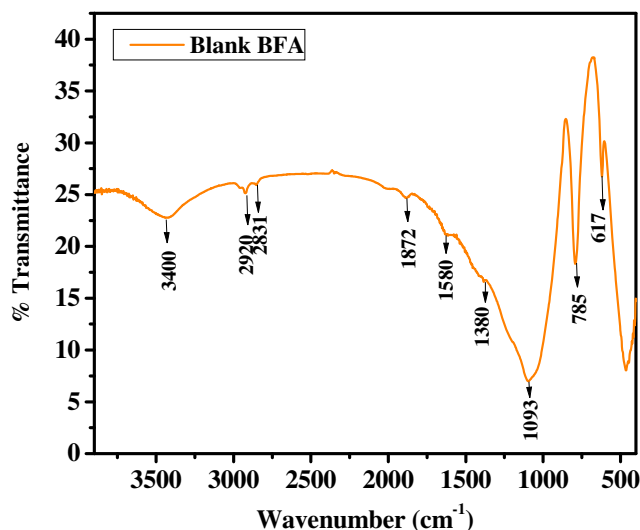


Fig. 1 FTIR of blank BFA

the presence of inorganic silicates. A sharp band at 785 cm^{-1} is due to the presence of Si–C. The presence of inorganic SO_4^{2-} ion is depicted by the presence of a band in a 617-cm^{-1} region (Stuart 2004, Smith 1998).

Nitrogen adsorption/desorption isotherms and the surface area characteristics for the BFA are provided in Fig. 2a. The apparent surface area was found to be $82.4\text{ m}^2/\text{g}$, and the adsorption average pore width (4 V/A by BET) of BFA was found to be 28.48 \AA . In the case of BFA, a hysteresis loop, which closes at a relative pressure around 0.4 (a type IV isotherm), is found. This indicates mesoporosity (Gregg and Sing 1982). From the isotherms, it can be inferred that the BFA have some microporosity in addition to mesoporosity.

Using the Harkins-Jura thickness equation (Harkins and Jura 1944), the analysis of the t-plot for BFA provides a micropore volume of $0.02\text{ cm}^3/\text{g}$ and a micropore surface area of $40.4\text{ m}^2/\text{g}$. This indicates that less than $\sim 50\%$ of the total apparent surface

area of the BFA comprises of micropores. The BJH analysis of BFA indicates the presence of mesopores (Fig. 2b).

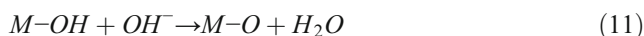
SEM micrographs of the blank BFA (Fig. 3a, b) display two different types of structures: (1) a fibrous structure which is carbon rich and (2) a SiO_2 -rich globular structure. After adsorption, the surface roughness of the carbon-rich BFA particles and silica globules increases due to the presence of colloids and particles in the wastewater (Fig. 3c). The EDX analysis of the BFA shows that silica and oxygen are present in a maximum amount followed by carbon. After the adsorption, the carbon and oxygen content of the loaded/spent BFA increased (Table 2). The proximate analysis of the BFA showed that it contains 4.6% moisture, 70.7% ash, 5.9% volatile matter, and 18.8% fixed carbon. The high concentration of ash shows that the BFA is basic in nature ($\text{pH}_{\text{PZC}} = 8.7$). The combustion of bagasse produces BFA having different amounts of carbon and silicon dioxide. The higher the temperature of the combustion, the lower will be the amount of the residual carbon. When the sample is heated at temperatures over $400\text{ }^\circ\text{C}$, nearly all of the carbon content is lost (Worathanakul et al. 2009).

Adsorption studies

Effect of initial pH

Batch adsorption studies were conducted with filtrate ($\text{COD} = 1650\text{ mg/L}$) at different initial pH ($2 \leq \text{pH}_i \leq 10$). Figure 4 shows the influence of initial pH (pH_i) of the filtrate on the COD removal with BFA at a dosage of 10 g/L , contact time $t = 3\text{ h}$, and at temperature = 298 K . Initial experimental runs showed that the COD removal from the wastewater did not increase significantly beyond 3 h of contact time with BFA. Therefore, a contact time of 3 h was determined as the time for adsorption equilibrium. At $\text{pH}_i = 4$, the COD removal efficiency of 58.2% was obtained.

The solution pH affects the degree of ionization and speciation of various compounds present in the wastewater. The pK_a are 3.51 and 4.82 for TA, 4.2 for BA, and 4.36 for *p*-toluic acid. At $\text{pH}_i 4$, TA and BA will be present as un-dissociated acid molecules. EDX analysis shows the presence of silica, calcium oxide, and aluminum oxide in the BFA (Table 2), which affect the BFA surface charge characteristics. The interaction between mineral oxides and water can be shown as follows:



where M may be Al, Ca, and Si. The pH_{PZC} of SiO_2 is 2.2. However, the pH_{PZC} (pH at the point of zero charge) is 8.3 for Al_2O_3 and 11 for CaO (Srivastava et al. 2006a). The adsorption of cations from the wastewater is favored when pH of wastewater is more than pH_{PZC} of BFA, while the adsorption of anions is favored at pH less than pH_{PZC} . A change in pH of

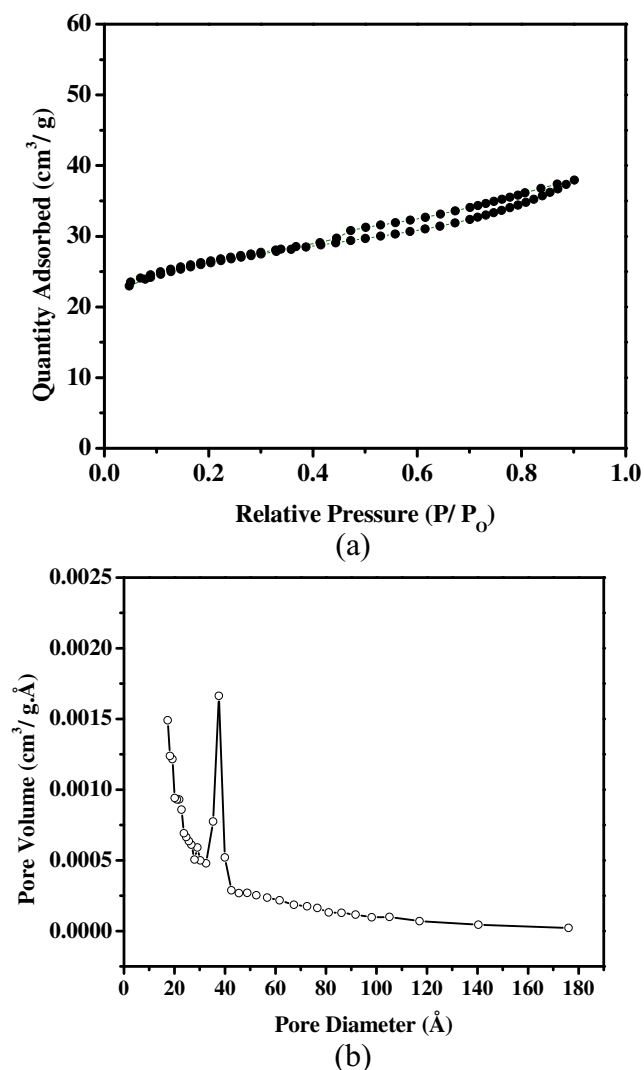
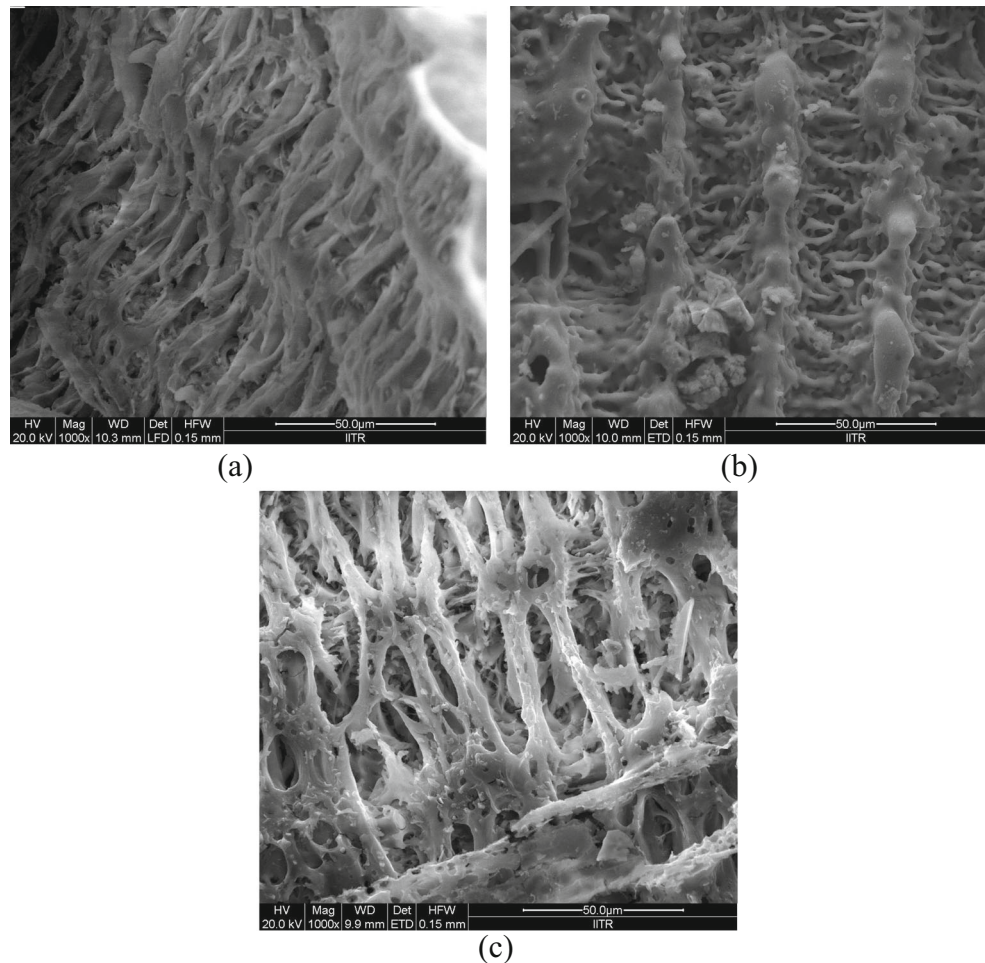


Fig. 2 a Nitrogen adsorption and desorption isotherms at 77 K. b BJH differential pore volume distributions for BFA

Fig. 3 SEM micrographs. **a, b** Blank. **c** Loaded BFA at 1000 \times magnification



the solution affects the adsorption process through dissociation of functional groups on the active sites of the surface of the BFA. The pH_{PZC} for BFA is 8.7. Thus, BFA is positively charged, as $pH_i < 8.7$. Thus, the electrostatic forces of attraction come into play between the negatively charged particles or colloids present in the wastewater and the positively charged surface of the BFA. Since the adsorption was conducted at a pH_i lower than pK_a of the solutes (TA, BA, and *p*-

toluic acid), the dispersive and dipolar interactions are the major adsorption forces, with the dipolar interaction being predominant (Jia et al. 2002; Haghseresht et al. 2002). As the initial pH of the wastewater was increased to the range

Table 2 EDX analysis of the BFA

Element (wt%)	Blank BFA	Loaded BFA
C	10.3	19.3
N	2.2	2.7
O	28.3	30.1
Al	1.9	2
Si	48.9	41.9
S	1	0.54
K	4.3	1.6
Ca	2.2	0.7
Fe	1.1	1.9

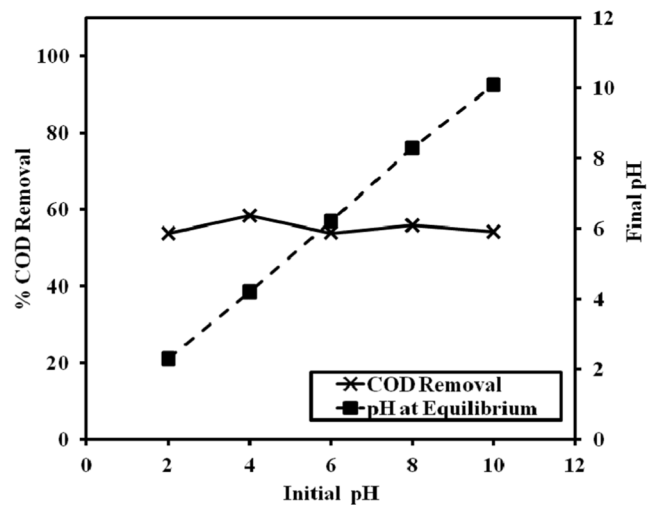


Fig. 4 Influence of initial pH on COD removal (BFA dosage = 10 g/L, contact time = 3 h, initial COD_i = 1650 mg/L, and temperature = 298 K)

6–10, no significant uptake of organics/inorganics from PTA wastewater was observed. As the pH_i of the system increased, the number of negatively charged sites increased and the number of positively charged sites decreased on the surface of BFA. A negatively charged surface site on the BFA did not favor the adsorption of anions due to electrostatic repulsion. This resulted in decreased adsorption of PTA wastewater components at pH range 6–12 in comparison to the removal at pH 4. Adhoum and Monser (2004) also made similar observations for the adsorption of PA by modified activated carbon. The system pH changes very little upwards during the adsorption process, and the equilibrium pH_{eq} remains almost the same as the pH_i value in the range of ($2 \leq pH_i \leq 10$) (Fig. 4).

The experiments were performed at the optimal pH_i 4, which is well below the pH_{PZC} of BFA. Therefore, more protons are contributed by the acidic PTA wastewater than hydroxide groups. A positive charge is generated on the BFA surface due to the attraction of protons to it. Due to the electrostatic attraction, the negatively charged particles from the wastewater get attached to the BFA. This results in a slight increase in the pH of the wastewater after adsorption.

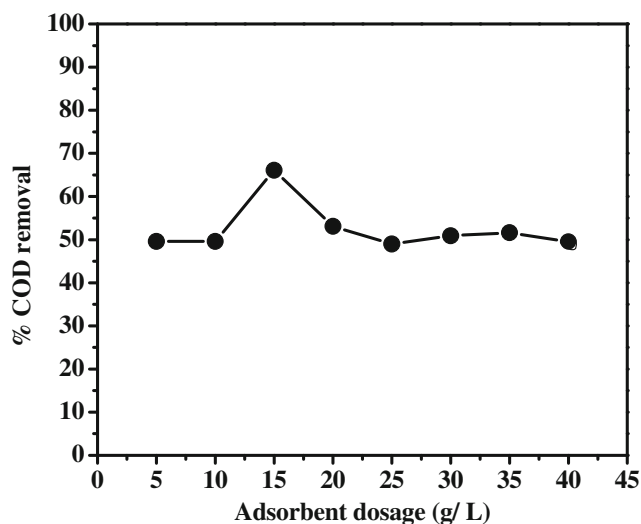
Effect of BFA dosage

The influence of adsorbent dosage (w) on the removal of COD from the wastewater was studied in the range of 5–40 g/L with an initial COD of 1650 mg/L and at $pH_i = 4$ and temperature 298 K. As the dosage of BFA was increased from 5 to 15 g/L, an increase in the COD removal was observed. As a high number of vacant adsorption sites are available at a high w , adsorptive removal of COD from PTA wastewater gets increased. However, beyond 15 g/L dosage of BFA, the COD removal decreased (Fig. 5a). This decrease in COD removal is mainly because of the adsorption sites remaining saturated during the adsorption process and the aggregation due to particle-particle interaction.

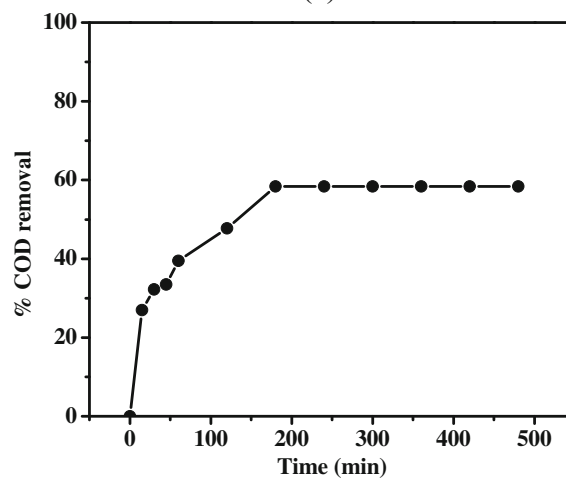
At the optimum adsorption treatment conditions, the COD of PTA wastewater gets reduced from 1650 to 690 mg/L, and the concentration of TA and BA get reduced from 27.3 to 1.01 mg/L and 109.3 to 0.06 mg/L, respectively. Thus, the adsorptive treatment of acid-pretreated PTA wastewater by BFA showed 58.2% removal of COD, 96.3% removal of TA and 99.9% removal of BA. This proves that the BFA is an effective adsorbent in removing TA and BA from the PTA wastewater.

Effect of contact time

Figure 5b shows the plot of COD removal versus contact time. It is found that the change in COD removal is not significant after 3 h of adsorption. A fast uptake of PTA wastewater components was seen during the initial 60 min for BFA, during which ~58% COD is removed. This fast uptake indicates the effectiveness of the BFA in COD removal. Initially, the



(a)



(b)

Fig. 5 Effect of **a** dosage and **b** contact time on COD removal by BFA ($w = 15$ g/L for BFA, $pH_i = 4.0$, initial $COD_i = 1650$ mg/L, and temperature = 298 K)

surface of BFA has a large number of unoccupied sites for the adsorption. Thereafter, the repulsive forces between the PTA wastewater (bulk liquid phase) and the wastewater components (TA, BA, *p*-toluic acid, acetic acid, etc.) on the surface of BFA become progressively stronger with time, making the occupation of vacant surface sites difficult. The resistance to transfer of PTA wastewater components from the bulk solution to the BFA pores also increases as they have to cover a larger transport path deeper into the pores. This increasing resistance retards the adsorption process at the later stages.

Adsorption kinetics

The frequently used kinetic models, viz. pseudo-first-order, pseudo-second-order, and the intraparticle diffusion models, have been tested to investigate the COD adsorption kinetics

Table 3 Kinetic parameters for the COD removal by BFA ($t = 3$ h, $\text{COD}_i = 1650$ mg/L, $w = 15$ g/L)

		Pseudo-first-order model (non-linear fitting)						
	$Q_{e(\text{exp})}$ (mg/g)	$Q_{e(\text{calc})}$ (mg/g)	K_1 (min^{-1})	r^2	RSS			
BFA	64	60.4	2.8	0.96	42.7			
		Pseudo-second-order model (non-linear fitting)						
	$Q_{e(\text{calc})}$ (mg/g)	K_2 [g/(mg min)]	h [mg/(g min)]	r^2	RSS			
BFA	62.5	6.9×10^{-4}	2.9	0.99	3.4			
		Intraparticle diffusion model (non-linear fitting)						
	K_{id1} [mg/(g min ^{1/2})]	Intercept I	r^2	RSS	K_{id2} [mg/(g min ^{1/2})]	Intercept II	r^2	RSS
BFA	0.23	29.69	0.994	2.67	2.5	63.5	0.99	7.5×10^{-5}

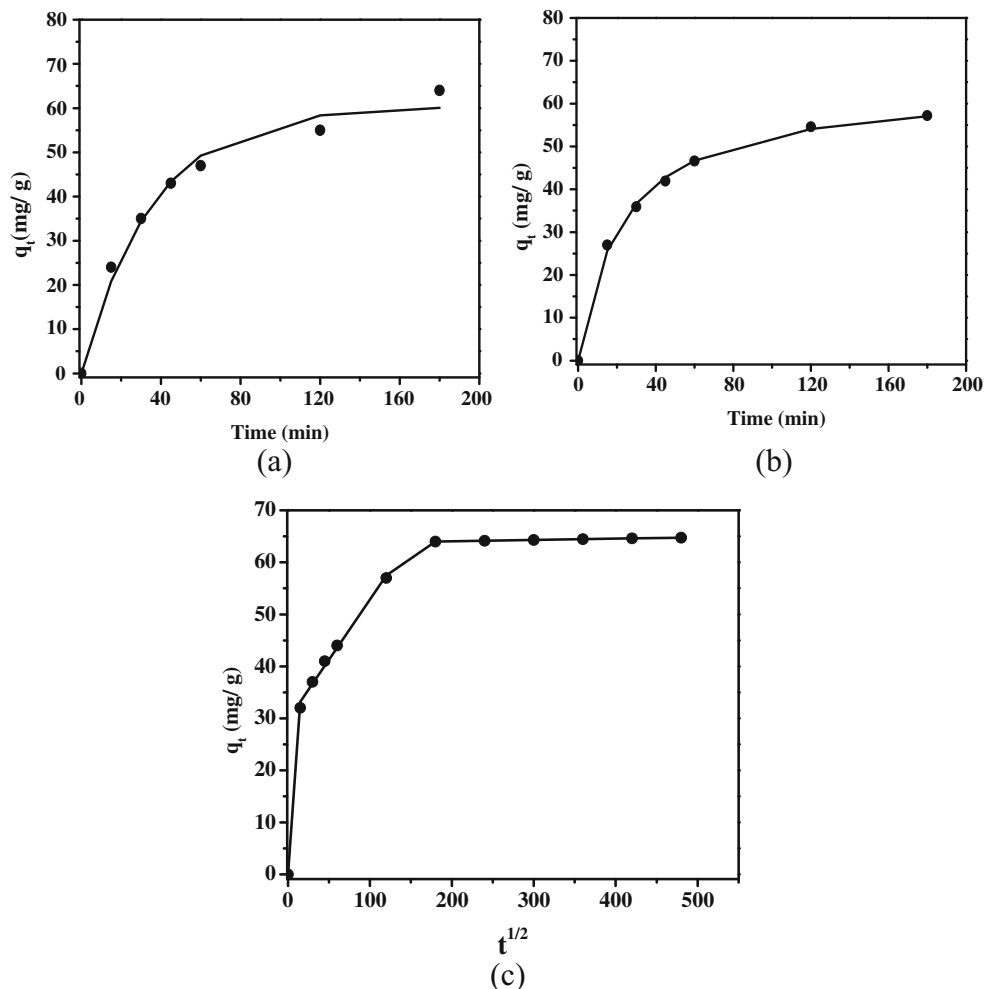
on BFA. The fitting of the experimental sorption data to the kinetic models was evaluated using the error analysis. To determine the best fit of the studied kinetic models to the COD adsorption data, correlation coefficient (R^2) and the residual sum of the squares of the errors (RSS) were examined. The values of R^2 and RSS are provided in Table 3.

The experimental adsorption data was found to be the poor fit to the pseudo-first-order-rate equation as shown in Fig. 6a and Table 3. The pseudo-first-order-rate equation is normally

confined to the initial stages of adsorption process. The application of this model for the longer adsorption periods and higher segmented surface coverage needs further modifications (Srivastava et al. 2006b). These factors contributed to low correlation coefficients and high RSS for BFA. Hence, the pseudo-first-order kinetics was rejected.

Figure 6a and Table 3 depict the non-linear fitting of experimental data with a pseudo-second-order kinetic equation. The pseudo-second-order-rate equation also yielded the

Fig. 6 Adaptation of experimental data on COD adsorption onto BFA to the **a** pseudo-first-order, **b** pseudo-second-order, and **c** intraparticle diffusion model ($t = 3$ h, $\text{COD}_i = 1650$ mg/L, $w = 15$ g/L for BFA)



model-calculated $q_{e (calc)}$ values close to the obtained experimental $q_{e (exp)}$ results. For pseudo-second-order kinetics, the value of R^2 is found to be close to unity and the RSS values are quite small. Therefore, the pseudo-second-order model best represents the sorption kinetics.

The transport of PTA wastewater components from the bulk liquid phase to the vacant adsorption sites of BFA is a multistep activity. Therefore, it is essential to recognize the slowest rate controlling step. In the rapidly stirred batch adsorption experiments, the boundary layer resistance diminishes. This creates a trivial difference between the concentration of wastewater components at the surface of the BFA and in the bulk solution (Srivastava et al. 2006b). Thus, the external mass transfer resistance can be neglected.

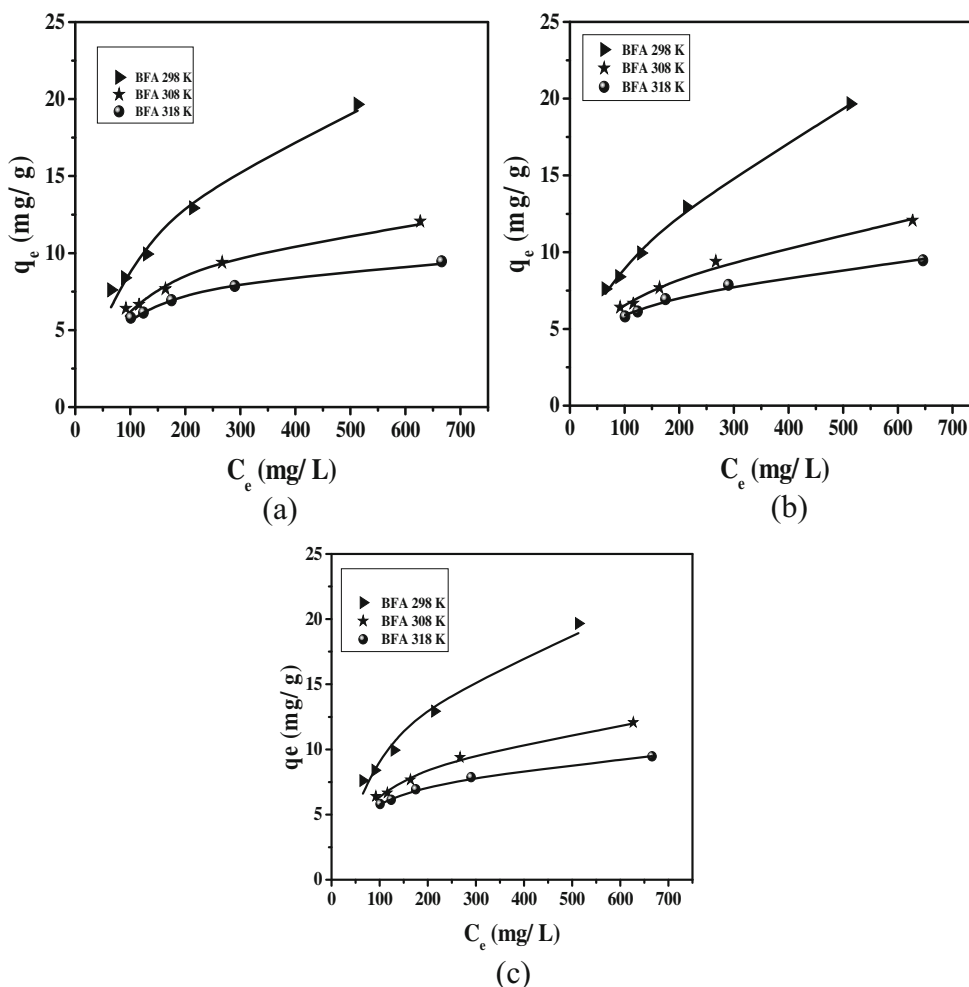
Figure 6c shows the fitting of experimental data to the intraparticle diffusion model. The data does not show a linear trend throughout the studied time period and also did not transverse the origin. The first linear portion of the graph depicts macropore/mesopore diffusion while the micropore diffusion is represented by the second linear portion of the graph. In the distinct regions of the graph, the rate of adsorption is

characterized by the rate parameters K_{id1} and K_{id2} . These rate parameters are defined by the slope of the linear portions of the graph. The intercepts of the extrapolated linear portion of the graph signify the boundary layer thickness. The larger the intercept, the greater is the boundary layer effect. The deviation of straight lines from the origin indicates that pore diffusion is not the sole rate controlling step in this adsorption process. The effective diffusivity, D_e , for various contaminants (represented by COD) on BFA is found to be $6.35 \times 10^{-14} \text{ m}^2/\text{s}$.

Adsorption isotherm study

The effect of temperature on the adsorption capacity of the BFA for PTA wastewater components was studied in the temperature range of 298 to 318 K. As the temperature increased, a decrease in adsorptivity of PTA wastewater components on BFA was observed. With an increase in temperature, the intermolecular forces between the adsorbate and the active sites of the solid surface become weak. Along with this, the dissolution of some of the components of PTA wastewater increases. Thus, the interactive forces between the water and PTA wastewater

Fig. 7 Equilibrium adsorption isotherm: amount of COD adsorbed on the adsorbent (q_e) versus residual COD concentrations (C_e): a Langmuir isotherm, b Freundlich isotherm, and c Temkin isotherm models ($t = 8 \text{ h}$, $\text{COD}_i = 165\text{--}1650 \text{ mg/L}$, BFA dosage = 15 g/L)



components become stronger in comparison to those between the BFA and PTA wastewater components. Therefore, a decrease in the adsorption of PTA wastewater components is evident with an increase in temperature. This effect indicates the exothermic nature of the adsorption process.

COD adsorption isotherm data starting at different COD concentrations were investigated to fit the isotherm models of Langmuir, Freundlich, and Temkin. The non-linear fit of these isotherm equations is shown in Fig. 7. These data were obtained by COD measurement after 3 h of contact time. Table 4 shows R² and RSS values for the Langmuir, Freundlich, and Temkin isotherms. The values of R² and RSS demonstrate a very good fit of the Freundlich isotherm model with the experimental data (Table 4). This shows that the BFA surface exhibits heterogeneity of the adsorption sites. This is also supported by the fact that the Langmuir isotherm, which is applicable for the homogeneous surface, does not fit well with the experimental adsorption data. The value of 1/n was found to be less than 1 for the Freundlich isotherm in the temperature range 298–318 K, favoring the occurrence of adsorption. However, the value of 1/n was found to increase from 0.26 to 0.48 as the temperature increased from 298 to 318 K. The value of K_F decreased with an increase in temperature. The exothermic nature of the adsorption process is exhibited by an increase in value of 1/n and a decrease in value of K_F. When the equilibrium concentration of adsorbate in liquid phase approaches C₀, the maximum adsorption capacity of BFA would be K_F C₀^{1/n}. In single stage adsorption, K_F C_e^{1/n} denotes the equilibrium adsorption capacity of BFA. The ratio of the maximum equilibrium adsorption capacity of BFA was (C₀/C_e)^{1/n}, which reaches up to 1.3. This shows the efficiency of BFA in adsorptive removal of PTA wastewater components.

Estimation of thermodynamic parameters for adsorption

The thermodynamic parameters such as ΔG⁰, ΔH⁰, and ΔS⁰ for the adsorption of PTA wastewater on BFA were also calculated. A decrease in ΔG⁰ was observed as the temperature increased (−1.4286, −0.8061, and −0.0263 kJ/mol at 298, 308, and 318 K, respectively). This indicates that the driving force responsible for adsorption has lowered resulting in the lowering of the adsorption capacity. The negative value of ΔG⁰ signifies that the sorption of wastewater constituents by BFA is spontaneous and feasible. The entropy change was also found to be negative (ΔS⁰ = −69.94 J/mol K). This indicates that at the solid/liquid interface, the degree of freedom decreases during the process of adsorption. The entropy of the solute due to adsorption is always negative. During adsorption, there is a rearrangement of water molecules enclosing the hydrophobic molecules. This rearrangement increases the system randomness, and the entropy of the PTA wastewater components lowers more than the increase in the entropy of the whole system. Therefore, the value of ΔS⁰ is found to be negative. The negative value of enthalpy change

Table 4 Isotherm parameters for the removal of COD by BFA (t = 3 h, COD_i = 1650–165 mg/L, w = 15 g/L)

Langmuir isotherm					
$qe = \frac{K_L q_m C_e}{1 + K_L C_e}$					
T (K)	K _L (L/mg)	q _m (mg/g)	r ²	RSS	
298	1.1 × 10 ⁻²	26.9	0.97	0.12	
BFA 308	7.6 × 10 ⁻³	14.3	0.98	0.4	
318	4.8 × 10 ⁻³	10.5	0.98	2.4	
Freundlich isotherm					
$q_e = K_F C_e^{1/n}$					
T (K)	K _F ((mg/g)/(L/mg))	1/n	r ²	RSS	
298	1.78	0.26	0.998	5.3 × 10 ⁻²	
BFA 308	1.37	0.34	0.994	0.14	
318	1.01	0.48	0.994	0.16	
Temkin isotherm					
$qe = \frac{RT}{b} \ln(C_e K_T) = B_T \ln(C_e K_T)$					
T (K)	K _T (l/mg)	B _T (kJ/mol)	r ²	RSS	
298	0.19	5.96	0.971	2.8	
BFA 308	8.01 × 10 ⁻²	3.06	0.992	0.16	
318	4.6 × 10 ⁻²	1.96	0.999	8.3 × 10 ⁻³	

where q_e is the equilibrium adsorption uptake (mg/g), K_L is the Langmuir adsorption constant, q_m signifies the adsorption capacity (mg/g), K_F is the Freundlich constant, 1/n is taken as the heterogeneity factor, B_T is related to the heat of adsorption, and K_T is the equilibrium binding constant

(ΔH⁰ = −22.3 kJ/mol) establishes the exothermic nature of the adsorption process. In physisorption, the range of adsorption energy is 5–10 kJ/mol. However, the range of adsorption energy is 30–70 kJ/mol for molecules and 100–400 kJ/mol for atoms in chemisorption process (Murzin and Salami 2005). The ΔH⁰ value of −22.3 kJ/mol for the present case is, perhaps, an indication of the occurrence of multilayer adsorption on the BFA surface. This also indicates that in the present

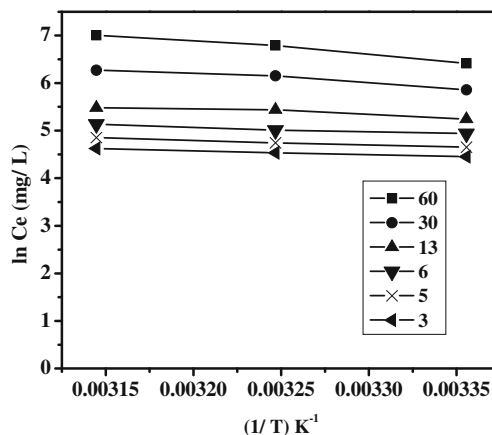


Fig. 8 Determination of isosteric enthalpy of adsorption for BFA at different q_e

study, the adsorption process cannot be considered completely either as physisorption or chemisorption. Thus, some different or a complex adsorption process may be occurring in this system (Mattson and Mark 1971).

Isosteric heat of adsorption

Figure 8 shows the isosteres corresponding to various q_e . The value of $\Delta H_{st,a}$ does not significantly vary with the surface loading. At q_e (mg/g) values of 60, 30, 13, 6, 5, and 3, the $\Delta H_{st,a}$ (kJ/mol) was found to be -22.1, -21.5, -21.1, -19, -18.98, and -18.8, respectively. This indicates that the surface of BFA is an energetically heterogeneous surface. This was also established by the best-fitting of the Freundlich model

with isotherm data. The negative values of $\Delta H_{st,a}$ indicate that adsorption process is exothermic in nature. An increase in $\Delta H_{st,a}$ value with an increase in q_e value was observed. At a low C_e value, there will be a direct interaction between the PTA wastewater components and BFA. Also a conducive adsorbate-adsorbate lateral interaction results in an increase in isosteric heat of adsorption (Al-Muhtaseb and Ritter 1999; Li et al. 2002; Martinez and Stern 2002).

Disposal of loaded BFA

BFA is available almost at no cost in comparison to other adsorbents such as activated carbon. Therefore, the regeneration of the exhausted BFA is not advised. The high silica

Table 5 Comparative assessment of COD removal from PTA wastewater

Properties	Adsorbents				
	GAC (Verma et al. 2014b)	BFA			
Surface characteristics					
pH _{pzc}	8.5	8.7			
Nature	Basic	Basic			
BET surface area(m ² /g)	134.6	82.4			
t-plot micropore area (m ² /g)	94.1	40.4			
t-plot micropore volume (cm ³ /g)	0.0487	0.0241			
Mesopore volume (cm ³ /g)	0.0284	0.0319			
Adsorption average pore width (4 V/A by BET) Å	24.4	28.5			
Particle size (mm)	1.5	0.45			
FTIR analysis	Inorganic silicates, OH groups, silanol groups, primary amine, γ (CO), aromatic compounds	Free and hydrogen-bonded OH groups, inorganic silicates, silanol groups, carboxyl-carbonate structures, aliphatic phosphorus, inorganic SO ₄ ²⁻ ion			
Optimum treatment conditions					
Adsorbent dosage (g/L)	20	15			
Temperature	Ambient	Ambient			
pH	4.0	4.0			
Adsorption kinetics and isotherms					
Best fitted kinetic model	Pseudo-second-order	Pseudo-second-order			
Best fitted isotherm model	Freundlich	Freundlich			
Overall adsorption process	Spontaneous and exothermic	Spontaneous and exothermic			
q_e (mg/g)	52.5	62.5			
Maximum equilibrium adsorption capacity(C0/Ce) ^{1/n}	1.22	1.3			
Removal at optimum treatment conditions					
Initial	After acid precipitation (mg/L)	Adsorption (mg/L)	% removal	Adsorption (mg/L)	% removal
COD (3530 mg/L)	1650	610	63%	690	58.2%
TA conc. (299 mg/L)	27.3	0.45	98.3%	1.01	96.3%
BA conc. (275 mg/L)	109.3	0.01	99.9%	0.06	99.9%
Disposal of loaded adsorbents			Regeneration, finally used after filtration and drying as a co-fuel. Heating value = 9.10 MJ/kg	No regeneration. After filtration and drying, either as a co-fuel or used in production of ceramic products and partial portland cement replacement	

content (as shown in EDX analysis) in the loaded BFA makes it a suitable raw material for making ceramic products such as insulation materials, membrane filters, and structural ceramics. Loaded BFA can also be added in mortar and concrete as a mineral blend. Some properties of the cementitious materials can be improved by partial replacement of portland cement with loaded BFA (Cordeiro et al. 2008).

Comparative assessment of COD removal efficiency of BFA with GAC from PTA wastewater

A comparative assessment of COD removal from PTA wastewater through BFA and GAC is provided in Table 5. Both the GAC and BFA are basic in nature. While the BFA displays a mesoporous structure, the GAC shows a microporous structure. At optimum adsorption treatment conditions, 63% removal of the COD was observed with GAC and 58.2% with BFA. Concentration of TA after adsorption was found to be 0.45 mg/L with GAC and 1.01 mg/L with BFA. The concentration of BA after adsorption with GAC and BFA was found to be 0.01 and 0.06 mg/L, respectively. This shows that the treatment of PTA wastewater by acid precipitation followed by adsorption results in 98.3 and 96.3% reduction in the concentration of TA and 99.9% reduction in the concentration of BA using GAC and BFA, respectively. This demonstrates that the adsorption efficiency of BFA is comparable to that of GAC. Thus, the BFA, being accessible almost at no cost and in abundance, has the advantage over GAC for PTA wastewater treatment (Verma et al. 2014b).

Two studies are reported in literature on the adsorptive removal of TA from synthetic wastewater. Anbia and Salehi (2012) found that the adsorption capacity (q_e) of CMK1/PDDA (surface area = 658.4 m²/g) for TA was 142.7 (mg/g) and 95.12 (mg/g) at the adsorbent dosage of 0.2 and 0.8 g/L, respectively. Caliskan et al. (2013) reported a very low adsorption capacity of 6.93 and 2.84 mg/g by TiO₂ and TiO₂-SiO₂ for TA, respectively. In the present study, the adsorption capacity of BFA was responsible for more than 95% removal of TA and BA and 58.2% removal of COD from the acid-pretreated PTA wastewater. The high removal of TA and BA make this wastewater suitable for biological treatment. These studies indicate that the BFA is a promising bio-waste material due to its reasonable adsorption capacity for the components of PTA wastewater.

Concluding remarks

BFA is found to be an effective adsorbent for the residual recalcitrant pollutant fraction of the PTA wastewater after acid pretreatment. At the optimum treatment conditions, COD is reduced by 58.35% with a 96.3% reduction in TA concentration and 99.9% reduction in BA concentration. The

Freundlich isotherm model was found to be the best fitted model for the adsorption of PTA wastewater components on to the BFA, and the adsorption process was exothermic and spontaneous in nature. These experimental results accentuate the possibility of application of BFA as an adsorbent for the wastewater treatment.

A comparative assessment of the removal efficiencies of GAC and BFA revealed that the concentration of TA after adsorption was found to be 0.45 and 1.01 mg/L, respectively. The concentration of BA after adsorption with GAC and BFA was found to be 0.01 and 0.06 mg/L, respectively. The ratio $(C_0/C_e)^{1/n}$ (maximum equilibrium adsorption capacity) was found to be 1.22 and 1.3 for GAC and BFA, respectively (Verma et al. 2014a). This indicated that both the GAC and BFA are comparable for their ability to absorb the components of PTA wastewater.

References

- Abou-Mesalam MM (2000) Adsorption kinetics of copper, zinc, cadmium and nickel ions on synthesized silico-antimonate ion exchanger. *Colloid Surface A* 225:85–94. doi:10.1016/S0927-7757(03)00191-2
- Adhoum N, Monser L (2004) Removal of phthalate on modified activated carbon: application to the treatment of industrial wastewater. *Separ Sci Technol* 38(3):233–239. doi:10.1016/j.seppur.2003.11.011
- Al-Muhtaseb SA, Ritter JA (1999) Roles of surface heterogeneity and lateral interactions on the isosteric heat of adsorption and adsorbed phase heat capacity. *J Phys Chem B* 103:2467–2479. doi:10.1021/jp984110s
- Anbia M, Salehi S (2012) Synthesis of polyelectrolyte-modified ordered nanoporous carbon for removal of aromatic organic acids from purified terephthalic acid wastewater. *Chem Eng Res Des* 90:975–983. doi:10.1016/j.cherd.2011.10.010
- APHA (American Public Health Association), AWWA (American Water Works Association), WPCF (Water Pollution Control Federation) (2003) Standard methods for the examination of water and wastewater. APHA, Washington, DC
- Ayranci A, Duman O (2006) Adsorption of aromatic organic acids onto high area activated carbon cloth in relation to wastewater purification. *J Hazard Mater* 136:542–552. doi:10.1016/j.jhazmat.2005.12.029
- Barrett EP, Joyner LG, Haldenda PH (1951) The determination of pore volume and area distributions in porous substances. I. Computations from nitrogen isotherms. *J Am Chem Soc* 73(1): 373–380. doi: 10.1021/ja01145a126
- Boehm HP (1966) Chemical identification of functional groups. In: Eley DD (ed) *Advances in catalysis*. Academic Press, New York
- Boyd GE, Adamson AW, Meyers LS (1947) The exchange adsorption of ions from aqueous solution by organic zeolites. II Kinetics *J Am Chem Soc* 69:2836–2848. doi:10.1021/ja01203a066
- Caliskan Ö, Doğan Ilgun A, Yilmazi M, Banu Yener H, Fehime Özkan S, Helvacı SS (2013) Adsorption behavior of terephthalic acid on TiO₂ nano particles synthesized by thermal hydrolysis method. Digital proceeding of the ICOEST'2013, Cappadocia. www.josunas.org/login/index.php/josunas/article/download/272/224
- Chen CY, Chen CC, Chung YC (2007) Removal of phthalate esters by α -cyclodextrin-linked chitosan bead. *Bioresour Technol* 98(13):2578–2583. doi:10.1016/j.biortech.2006.09.009

- Chen CY, Chung YC (2006) Removal of phthalate esters from aqueous solution by chitosan bead. *J Environ Sci Heal A* 41(2):235–248. doi:10.1080/10934520500354573
- Cordeiro GC, Toledo Filho RD, Tavares LM, Fairbairn EMR (2008) Pozzolanic activity and filler effect of sugar cane bagasse ash in portland cement and lime mortars. *Cem Concr Compos* 30:410–418. doi:10.1016/j.cemconcomp.2008.01.001
- Dulazi AA, Liu H (2011) Removal of phthalate esters from water using immobilized lipase on chitosan beads. *Environ Technol* 32(13):1443–1451. doi:10.1080/09593330.2010.538932
- Garg A, Mishra IM, Chand S (2010) Effectiveness of coagulation and acid precipitation processes for the pre-treatment of diluted black liquor. *J Hazard Mater* 180(1–3):158–164. doi:10.1016/j.jhazmat.2010.04.008
- Gilarranz MA, Rodriguez F, Oliet M, Reveng JA (1998) Acid precipitation and purification of wheat straw lignin. *Separ Sci Technol* 33(9):1359–1377. doi:10.1080/01496399808544988
- Gregg SJ, Sing KSW (1982) Adsorption, surface area and porosity, 2nd edn. London
- Haghsereht F, Nouri S, Finnerty JJ, Lu GQ (2002) Effects of surface chemistry on aromatic compound adsorption from dilute aqueous solutions by activated carbon. *J Phys Chem B* 106(42):10935–10943. doi:10.1021/jp025522a
- Harkins WD, Jura G (1944) Surfaces of solids. XIII. A vapor adsorption method for the determination of the area of a solid without the assumption of a molecular area, and the areas occupied by nitrogen and other molecules on the surface of a solid. *J Am Chem Soc* 66:1366–1373. doi:10.1021/ja01236a048
- Hauser R, Calafat AM (2005) Phthalates and human health. *Occup Environ Med* 62:806–818. doi:10.1136/oem.2004.017590
- Heudorf U, Mersch-Sundermann V, Angerer J (2007) Phthalates: toxicology and exposure. *Int J Hyg Environ Health* 210:623–634. doi:10.1016/j.ijheh.2007.07.011
- Jia YF, Xiao B, Thomas KM (2002) Adsorption of metal ions on nitrogen surface functional groups in activated carbons. *Langmuir* 18(2):470–478. doi:10.1021/la011161z
- Joung JY, Lee HW, Choi H, Lee MW, Park JM (2009) Influences of organic loading disturbances on the performance of an aerobic filter process to treat purified terephthalic acid wastewater. *Bioresour Technol* 100:2457–2461. doi:10.1016/j.biortech.2008.11.034
- Karthik M, Dafale NP, Pathe PT, Nandy T (2008) Biodegradability enhancement of purified terephthalic acid wastewater by coagulation–flocculation process as pretreatment. *J Hazard Mater* 154:721–730. doi:10.1016/j.jhazmat.2007.10.085
- Kleerebezem R, Hulshoff Pol LW, Lettinga G (1999a) Anaerobic biodegradability of phthalic acid isomers and related compounds. *Biodegradation* 10(1):63–73. doi:10.1023/A:1008321015498
- Kleerebezem R, Hulshoff Pol LW, Lettinga G (1999b) The role of benzoate in anaerobic degradation of terephthalate. *Appl Environ Microbiol* 65(3):1161–1167
- Lataye DH, Mishra IM, Mall ID (2006) Removal of pyridine from aqueous solution by adsorption on bagasse fly ash. *Ind Eng Chem Res* 45:3934. doi:10.1021/ie051315w
- Lataye DH, Mishra IM, Mall ID (2008) Pyridine sorption from aqueous solution by rice husk ash (RHA) and granular activated carbon (GAC): parametric, kinetic, equilibrium and thermodynamic aspects. *J Hazard Mater* 154:858–870. doi:10.1016/j.jhazmat.2007.10.111
- Li A, Zhang Q, Zhang G, Chen J, Fei Z, Liu F (2002) Adsorption of phenolic compounds from aqueous solutions by a water-compatible hypercrosslinked polymeric adsorbent. *Chemosphere* 47:981–989. doi:10.1016/S0045-6535(01)00222-3
- Long C, Lu J, Li A, Zhang Q (2009) Removal of endocrine disrupting chemicals from aqueous phase using spherical microporous carbon prepared from waste polymeric exchanger. *Water Sci Technol* 60(6):1607–1614. doi:10.2166/wst.2009.495
- Lyche JL, Gutleb AC, Bergman A, Eriksen GS, Murk ATJ, Ropstad E, Saunders M, Skaare JU (2009) Reproductive and developmental toxicity of phthalates. *J Toxicol Environ Heal B* 12:225–249. doi:10.1080/10937400903094091
- Martinez S, Stern I (2002) Thermodynamic characterization of metal dissolution and inhibitor adsorption processes in the low carbon steel/ mimosin/ sulfuric acid system. *Appl Surf Sci* 199:83–89. doi:10.1016/S0169-4332(02)00546-9
- Mattson JS, Mark Jr HB (1971) Activated carbon: surface chemistry and adsorption from solution. New York
- Meeker JD, Sathyanarayana S, Swan SH (2009) Phthalates and other additives in plastics: human exposure and associated health outcomes. *Phil Trans R Soc B* 364:2097–2113. doi:10.1098/rstb.2008.0268
- Murzin D, Salami T (2005) Chemical kinetics. Elsevier, Amsterdam
- Nevskaia DM, Castillejos-Lopez E, Guerrero-Ruiz A, Munoz V (2004) Effects of the surface chemistry of carbon materials on the adsorption of phenol–aniline mixtures from water. *Carbon* 42(3):653–665. doi:10.1016/j.carbon.2004.01.007
- Park TJ, Lima JS, Lee YW, Kim SH (2003) Catalytic supercritical water oxidation of wastewater from terephthalic acid manufacturing process. *J Supercrit Fluid* 26:201–213. doi:10.1016/S0896-8446(02)00161-4
- Pillai KC, Kwon TO, Moon IS (2009) Degradation of wastewater from terephthalic acid manufacturing process by ozonation catalyzed with Fe²⁺, H₂O₂ and UV light: direct versus indirect ozonation reactions. *Appl Catal B* 91:319–328. doi:10.1016/j.apcatb.2009.05.040
- Pophali GR, Khan R, Dhodapkar RS, Nandy T, Devotta S (2007) Anaerobic–aerobic treatment of purified terephthalic acid (PTA) effluent: a techno-economic alternative to two-stage aerobic process. *J Environ Manag* 85:1024–1033. doi:10.1016/j.jenvman.2006.11.016
- Rivas FJ, Beltrán F, Carvalho F, Acedo B, Gimeno O (2004) Stabilized leachates: sequential coagulation–flocculation + chemical oxidation process. *J Hazard Mater B* 116:95–102. doi:10.1016/j.jhazmat.2004.07.022
- Shafaei AM, Nikazar M, Arami M (2010) Photocatalytic degradation of terephthalic acid using titania and zinc oxide photocatalysts: comparative study. *Desalination* 252:8–16. doi:10.1016/j.desal.2009.11.008
- Smith BC (1998) Infrared spectral interpretation: a systematic approach. CRC Press. ISBN 9780849324635
- Srivastava VC, Mall ID, Mishra IM (2006b) Characterization of mesoporous rice husk ash (RHA) and adsorption kinetics of metal ions from aqueous solution onto RHA. *J Hazard Mater* 134:257–267. doi:10.1016/j.jhazmat.2005.11.052
- Srivastava VC, Mall ID, Mishra IM (2007) Adsorption thermodynamics and isosteric heat of adsorption of toxic metal ions onto bagasse fly ash (BFA) and rice husk ash (RHA). *Chem Eng J* 132:267–278. doi:10.1016/j.cej.2007.01.007
- Srivastava VC, Swamy MM, Mall ID, Prasad B, Mishra IM (2006a) Adsorptive removal of phenol by bagasse fly ash and activated carbon: equilibrium, kinetics and thermodynamics. *Colloid Surface A* 272:89–104. doi:10.1016/j.colsurfa.2005.07.016
- Stuart BH (2004) Infrared spectroscopy: fundamentals and applications, John Wiley
- Swan SH (2008) Environmental phthalate exposure in relation to reproductive outcomes and other health endpoints in humans. *Environ Res* 108:177–184. doi:10.1016/j.envres.2008.08.007
- Thiruvenkatachari R, Kwon TO, Jun JC, Balaji S, Matheswaran M, Shik Moon I (2007) Application of several advanced oxidation processes for the destruction of terephthalic acid (TPA). *J Hazard Mater* 142:308–314. doi:10.1016/j.jhazmat.2006.08.023
- Tsang PK, Fang ZQ, Liu H, Chen X (2008) Kinetics of adsorption of di-n-butyl phthalate (DBP) by four different granule-activated carbons. *Front Chem Chin* 23(3):288–293. doi:10.1007/s11458-008-0064-6

- Verma S, Prasad B, Mishra IM (2010) Pretreatment of petrochemical wastewater by coagulation and flocculation and the sludge characteristics. *J Hazard Mater* 178:1055–1064. doi:10.1016/j.jhazmat.2010.02.047
- Verma S, Prasad B, Mishra IM (2014a) Treatment of petrochemical wastewater by acid precipitation and carbon adsorption. *J Hazard Toxic Radioact Waste* 18(3):04014013. doi:10.1061/(ASCE)HZ.2153-5515.0000219
- Verma S, Prasad B, Mishra IM (2014b) Adsorption kinetics and thermodynamics of COD removal of acid treated petrochemical wastewater by using granular activated carbon. *Separ Sci Technol* 49(7):1067–1075
- Vermeulen T (1953) Theory for irreversible and constant pattern solid diffusion. *Ind Eng Chem* 45(8):1664–1670. doi:10.1021/ie50524a025
- Wen YZ, Tong SP, Zheng KF, Wang LL, Lv JZ, Lin J (2006) Removal of terephthalic acid in alkalized wastewater by ferric chloride. *J Hazard Mater* 138:169–172. doi:10.1016/j.jhazmat.2006.05.070
- Wittcoff HA, Reuben BG, Plotkin JS (2004) *Industrial organic chemicals*, 2nd edn. Wiley-Interscience
- Worathanakul P, Payubnop W, Muangpet A (2009) Characterization for post-treatment effect of bagasse ash for silica extraction. *World Acad Sci Eng Technol* 56:360–362
- Xu Z, Zhang W, Pan B, Lv L, Jiang Z (2011) Treatment of aqueous diethyl phthalate by adsorption using a functional polymer resin. *Environ Technol* 32(2):145–153. doi:10.1080/09593330.2010.490854
- Zhang Z, Ma L, Zhang XX, Li W, Zhang Y, Wu B, Yang L, Cheng S (2010) Genomic expression profiles in liver of mice exposed to purified terephthalic acid manufacturing wastewater. *J Hazard Mater* 181:1121–1126. doi:10.1016/j.jhazmat.2010.05.131
- Zhuravlev LT (1987) Concentration of hydroxyl groups on the surface of amorphous Silicas. *Langmuir* 1987(3):316–318. doi:10.1021/la00075a004